Termination of cAMP signals by Ca^{2+} and $G\alpha_i$ via extracellular Ca^{2+} sensors: a link to intracellular Ca^{2+} oscillations

Andrea Gerbino,[1,2] Warren C. Ruder,[1] Silvana Curci,[1,2] Tullio Pozzan,[3] Manuela Zaccolo,[4] and Aldebaran M. Hofer[1,2]

[1]Veterans' Affairs Boston Healthcare System, West Roxbury, MA 02132
[2]Department of Surgery, Brigham and Women's Hospital, Harvard Medical School, Boston, MA 02115
[3]Department of Biomedical Sciences, Venetian Institute of Molecular Medicine, University of Padua, 35129 Padua, Italy
[4]Dulbecco Telethon Institute, Venetian Institute of Molecular Medicine, 35129 Padua, Italy

Termination of cyclic adenosine monophosphate (cAMP) signaling via the extracellular Ca^{2+}-sensing receptor (CaR) was visualized in single CaR-expressing human embryonic kidney (HEK) 293 cells using ratiometric fluorescence resonance energy transfer–dependent cAMP sensors based on protein kinase A and Epac. Stimulation of CaR rapidly reversed or prevented agonist-stimulated elevation of cAMP through a dual mechanism involving pertussis toxin–sensitive $G\alpha_i$ and the CaR-stimulated increase in intracellular $[Ca^{2+}]$. In parallel measurements with fura-2, CaR activation elicited robust Ca^{2+} oscillations that increased in frequency in the presence of cAMP, eventually fusing into a sustained plateau. Considering the Ca^{2+} sensitivity of cAMP accumulation in these cells, lack of oscillations in [cAMP] during the initial phases of CaR stimulation was puzzling. Additional experiments showed that low-frequency, long-duration Ca^{2+} oscillations generated a dynamic staircase pattern in [cAMP], whereas higher frequency spiking had no effect. Our data suggest that the cAMP machinery in HEK cells acts as a low-pass filter disregarding the relatively rapid Ca^{2+} spiking stimulated by Ca^{2+}-mobilizing agonists under physiological conditions.

Introduction

cAMP controls crucial physiological cell functions such as cell growth, differentiation, transcriptional regulation, and apoptosis. Levels of intracellular cAMP principally reflect a balance between synthesis of the second messenger by adenylyl cyclases (ACs; activated through G protein–coupled receptors [GPCRs] coupled to $G\alpha_s$), degradation by phosphodiesterases (PDEs), and the inhibitory action of pertussis toxin (PTX)–sensitive $G\alpha_i$-coupled receptors that serve to limit cAMP formation by AC. The classical intracellular effector of the cAMP signal is protein kinase A (PKA), a holotetrameric complex that consists of two regulatory and two catalytic subunits that dissociate upon cAMP binding. More recently, a second class of intracellular cAMP targets has been identified: Epacs (exchange proteins activated by cAMP) are monomeric proteins that undergo significant conformational changes upon cAMP binding, allowing them to activate their target, Rap1 (Beavo and Brunton, 2002). Aberrations in cAMP signaling or inappropriate cAMP production can have serious pathological consequences (e.g., tumor formation and heart failure). Therefore, understanding how cAMP signals are terminated is just as important as understanding how they are generated in the first place.

In addition to inhibition through the classical PTX-sensitive $G\alpha_i$, intracellular Ca^{2+} signaling pathways can exert powerful modulatory actions on cAMP accumulation (for review see Bruce et al., 2003). For example, some members of the extensive superfamily of PDEs (particularly those belonging to the PDE1 family) are activated by elevated intracellular Ca^{2+} (Houslay and Milligan, 1997; Goraya et al., 2004). In addition, specific isoforms of AC have been shown to respond to physiological changes in intracellular Ca^{2+} with either activation or inhibition of enzymatic activity (de Jesus Ferreira et al., 1998; Chabardes et al., 1999; Cooper, 2003). Ca^{2+} entering the cell via store-operated channels preferentially regulates cAMP

A. Gerbino's present address is Dipartimento di Fisiologia Generale ed Ambientale, Universita' di Bari, 70126 Bari, Italy.

Correspondence to Aldebaran M. Hofer: ahofer@rics.bwh.harvard.edu

Abbreviations used in this paper: AC, adenylyl cyclase; $[Ca^{2+}]_i$, intracellular calcium concentration; CaR, extracellular Ca^{2+}-sensing receptor; Epac, exchange protein activated by cAMP; FRET, fluorescence resonance energy transfer; GPCR, G protein–coupled receptor; HEK, human embryonic kidney; $InsP_3$, inositol 1,4,5-trisphosphate; PDE, phosphodiesterase; PGE_2, prostaglandin E_2; PKA, protein kinase A; PTX, pertussis toxin; VIP, vasoactive intestinal peptide; WT, wild-type.

The Journal of Cell Biology, Vol. 171, No. 2, October 24, 2005 303–312
http://www.jcb.org/cgi/doi/10.1083/jcb.200507054

production by AC and has been proposed to be much more effective than Ca^{2+} released from intracellular stores or influx via other types of Ca^{2+} channels (Cooper, 2003).

Conversely, the cAMP pathway can influence Ca^{2+} signaling at many levels. For example, PKA-dependent phosphorylation of intracellular release channels, such as the inositol 1,4,5-trisphosphate ($InsP_3$) receptor, and Ca^{2+} extrusion mechanisms, such as the plasma membrane Ca^{2+} ATPase, can powerfully shape Ca^{2+} signals (for review see Bruce et al., 2003). Reciprocal modulation by cAMP and Ca^{2+} pathways will be expected to generate unique patterns of signaling molecules during concurrent activation of receptors linked to each of these signal transduction cascades.

Agonist-induced oscillations in intracellular ($[Ca^{2+}]_i$) are a well-described phenomenon. Based on the fact that intracellular Ca^{2+} can augment or inhibit cAMP accumulation, it is predicted that cAMP levels would fluctuate during oscillatory Ca^{2+} spiking in a cell type in which Ca^{2+}-dependent ACs or PDEs were expressed (Cooper et al., 1995). Repetitive activation–inactivation cycles of the cAMP signaling pathway could conceivably encode information that differed from large static changes in the second messenger. Precisely this sort of regulation has been shown to be operative for Ca^{2+} in cells displaying oscillatory Ca^{2+} signaling events. The frequency, amplitude, and duration of Ca^{2+} spiking are known to differentially regulate key cellular functions such as gene transcription and the activation of plasma membrane ion channels (Thorn et al., 1993; Dolmetsch et al., 1998; Berridge et al., 2000).

In the present study we examined the interactions of the extracellular Ca^{2+}-sensing receptor (CaR) with the cAMP signal transduction cascade. This widely expressed dimeric GPCR was first cloned more than a decade ago from bovine parathyroid cells (Brown et al., 1993). Since that time, expression of CaR has been demonstrated in several epithelial, glial, and neuronal cell types. CaR is able to sense small fluctuations in the extracellular $[Ca^{2+}]$ within the physiological range (Brown and MacLeod, 2001). Interestingly, this receptor is not strictly a calcium sensor, as it can be stimulated by a variety of physiologically relevant divalent and polycationic compounds. These compounds include Mg^{2+}; amino acids; and polyamines, such as spermine and spermidine. CaR can also be activated through allosteric modulation by synthetic small molecule "calcimimetics," such as NPS-R-467 (Conigrave et al., 2000; Hofer and Brown, 2003; Breitwieser et al., 2004; Nemeth, 2004).

In CaR-transfected human embryonic kidney (HEK) 293 cells (HEK CaR) and in several other cell models in which the receptor is expressed endogenously, CaR stimulation leads to robust oscillations in $[Ca^{2+}]_i$ (Breitwieser and Gama, 2001; Young and Rozengurt, 2002; De Luisi and Hofer, 2003). In addition to this coupling to the phosphoinositide–$InsP_3$–Ca^{2+} signaling pathway via $G\alpha_{q/11}$, CaR has also been shown to inhibit cAMP production (as measured using standard biochemical techniques) through interactions with PTX-sensitive proteins, presumably $G\alpha_i$ (Chen et al., 1989; Chang et al., 1998). In the present study we used recently introduced fluorescence resonance energy transfer (FRET)–based fluorescent indicators for cAMP that allowed us to visualize the inhibitory actions of CaR activation on cAMP levels in single living HEK CaR cells in real time (Zaccolo and Pozzan, 2002; Ponsioen et al., 2004). Our data confirm that CaR interacts with PTX-sensitive $G\alpha_i$ to inhibit AC in cells stimulated with cAMP-generating agonists (prostaglandin E_2 [PGE_2], vasoactive intestinal peptide [VIP], and isoproterenol).

Pharmacological and Western blot evidence suggest that HEK 293 cells express principally Ca^{2+}-insensitive isoforms of PDE (specifically, PDE4D3 and PDE4D5; Hoffmann et al., 1999; Rich et al., 2001b). These cells are also known to express multiple isoforms of AC (AC1, 3, 5, 6, 7, and 9 and soluble, bicarbonate-sensitive AC; Wayman et al., 1995; Ludwig and Seuwen, 2002; Geng et al., 2005), of which some are Ca^{2+} inhibitable (e.g., AC5 and AC6) and others are activated by Ca^{2+} or Ca^{2+}/calmodulin (e.g., AC1; soluble, bicarbonate-sensitive AC; and possibly AC3). Because these enzyme subtypes may have antagonistic actions on cAMP accumulation, it is difficult to predict the effects of intracellular Ca^{2+} elevations on cAMP signaling. In this study we found that $[Ca^{2+}]_i$ increases had a substantial inhibitory effect on cAMP levels, suggesting the prevailing action to be on Ca^{2+}-inhibitable AC. We also found that in the presence of elevated cAMP, agonist-stimulated Ca^{2+} signaling is further augmented, providing additional inhibitory feedback on cAMP generation. These factors conspire to make CaR a particularly potent antagonist of cAMP generation.

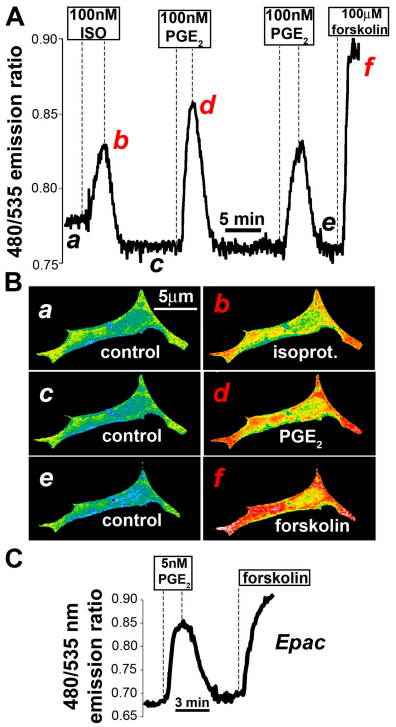

Figure 1. **Changes in the 480/535 nm FRET emission ratio in HEK CaR cells expressing cAMP sensors in response to cAMP-elevating agonists.** (A) Cells expressing the PKA-based sensor (R-CFP + C-YFP) were stimulated with 100 nM isoproterenol (ISO), 100 nM PGE_2, and 100 μM forskolin. (B) Ratio images corresponding to the time points (a–f) indicated in the trace in A. The probe was excluded from the nuclear compartment, although in this nonconfocal image, a signal emanating from above and below the nucleus gives the appearance of a nuclear ratio change. (C) Response of cells expressing Epac-based sensor to 5 nM PGE_2 and 100 μM forskolin.

Because CaR agonists reliably elicit robust oscillations in intracellular Ca^{2+} in HEK CaR cells, we reasoned that [cAMP] might also oscillate during CaR activation. However, although both the amplitude and frequency of Ca^{2+} oscillations, as measured by fura-2, were initially markedly enhanced by cAMP, these Ca^{2+} spikes were observed to eventually fuse into a sustained plateau of elevated [Ca^{2+}]. At the same time, experiments using the PKA probe and a system of artificially generated Ca^{2+} pulses revealed that dissociation of PKA (the major intracellular target of the cAMP signal) is indifferent to patterns of rapid Ca^{2+} spiking, such as those elicited by an agonist in the absence of cAMP. In contrast, in the face of low-frequency, long-duration Ca^{2+} oscillations, a complex, descending staircase pattern of cAMP (as measured by PKA dissociation) was unmasked. These results show that the cAMP signaling machinery in HEK cells can discriminate between different patterns of Ca^{2+} oscillations and is, in principle, immune to the rapid spiking stimulated physiologically by Ca^{2+}-mobilizing agonists.

Results

Characterization of the cAMP probe in HEK 293 CaR cells

Several different types of fluorescent cAMP sensors have been described previously (Adams et al., 1991; Zaccolo et al., 2000; Zaccolo and Pozzan, 2002; DiPilato et al., 2004; Mongillo et al., 2004; Ponsioen et al., 2004; Landa et al., 2005). Here we used recently developed FRET sensors based on PKA (Zaccolo and Pozzan, 2002) and Epac (Ponsioen et al., 2004) to continuously monitor cAMP levels for extended periods of time in single HEK CaR cells. Fig. 1 A shows that stimulation of endogenous β-adrenoceptors using 100 nM isoproterenol produced rapid and reversible elevation in the FRET ratio. Repeated stimulation of prostanoid receptors (EP_2/EP_4) with 100 nM of the inflammatory mediator PGE_2 yielded largely reproducible responses in the same cell. This agonist dose generally caused ratio responses that were smaller than the saturating activation elicited by a supramaximal dose (100 μM) of forskolin. This stimulation protocol was therefore used for much of the remainder of the study (typical of results from 32 cells in five experiments). Fig. 1 B shows pseudocolor images of the 480/535 nm FRET emission ratio of the PKA-based sensor, corresponding to the plot shown in Fig. 1 A. CFP- and YFP-labeled PKA subunits were distributed throughout the cytoplasm in transfected cells but were excluded from the nuclear compartment (not depicted). Significantly, because of the high sensitivity of these FRET-based techniques, we were able to detect ratio changes in response to low nanomolar concentrations of cAMP-generating agonists (e.g., 6.25 nM VIP or 10 nM isoproterenol; not depicted). One drawback, in fact, of the high sensitivity of these probes is that it is possible to saturate the indicators when GFP-tagged PKA subunits are dissociated to the maximal extent, even though intracellular cAMP continues to rise. This issue is discussed further on the following page. We also used a second type of cAMP probe based on Epac that exhibits a faster response time (Ponsioen et al., 2004). As illustrated in Fig. 1 C, reversible ratio changes after stimulation with 5 nM PGE_2 were readily discriminated in HEK CaR cells using this sensor.

Role of CaR in terminating cAMP signaling

We next took advantage of the extraordinary sensitivity of these cAMP indicators to examine how activation of CaR influenced cAMP signaling. Fig. 2 A shows that the elevation of the emission ratio induced by 100 nM PGE_2 was completely abolished by brief preexposure to NPS-R-467, a specific synthetic allosteric activator of CaR (n = 38 cells in six experiments; Nemeth, 2004). This calcimimetic by itself did not have any effect on cAMP levels, as measured by FRET. The data in Fig. 2 B further support this result. In the presence of the CaR agonist spermine, an extremely high dose (3 μM) of PGE_2 produced only a very small transient increase in the ratio, followed by a small undershoot, showing that CaR is extremely effective in inhibiting cAMP production. The cAMP signal was partially recovered after spermine washout. Prestimulation of CaR with spermine or 3 mM Ca^{2+} was able to completely abolish the ratio increase when a lower dose (100 nM) of PGE_2 was applied

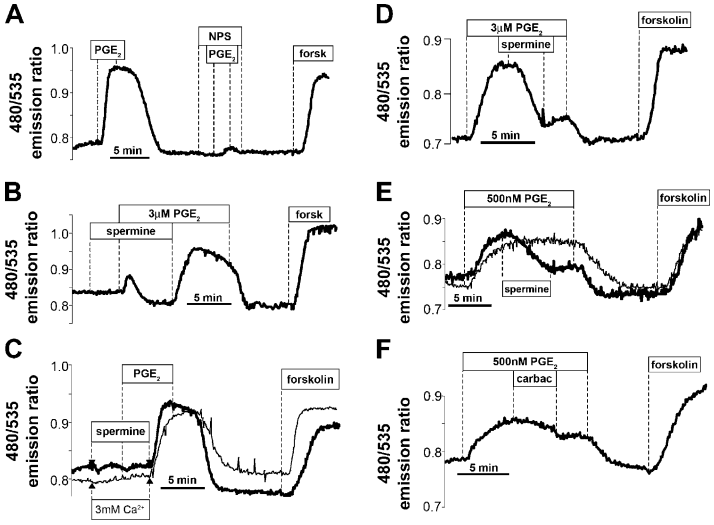

Figure 2. **Stimulation of HEK CaR cells with CaR agonists prevents or reverses PGE_2-induced cAMP formation as measured by the 480/535 nm emission ratio of PKA sensors.** (A) Response to 100 nM PGE_2 is prevented by 5 μM of the specific synthetic CaR modulator NPS-R-476. (B) Another CaR agonist, spermine (used at 1 mM throughout this study), largely inhibited the ratio change elicited by a supramaximal dose (3 μM) of PGE_2; comparison with response to 100 μM forskolin. (C) Similarly, spermine or 3 mM Ca^{2+} completely blocked response to a lower dose (100 nM) of PGE_2. (D) Acute addition of spermine during stimulation with 100 nM PGE_2 reverses the ratio elevation. (E) Experiments using the low-affinity cAMP indicator R230K show smooth nonoscillatory decline in FRET ratio during acute spermine (1 mM) treatment (bold trace); the thinner line represents control recording. (F) Comparison with the action of the Ca^{2+}-mobilizing agonist 100 μM carbachol. Experiments using the low-affinity cAMP indicator R230K show a significantly reduced action on the FRET ratio during acute carbachol treatment compared with spermine treatment.

(Fig. 2 C; $n = 16/19$ cells in four experiments for spermine, and $n = 15/15$ cells in three experiments for 3 mM Ca^{2+}). Thus, preexposure to a variety of CaR agonists effectively prevented the increase in cAMP production.

CaR stimulation was also able to reverse cAMP generation in cells previously stimulated with PGE_2 or other agonists. Spermine addition at the peak of the PGE_2-induced cAMP elevation caused a reversal of the ratio, as measured with this PKA-based probe (Fig. 2 D; $n = 69$ cells in eight experiments). However, we noted that in some experiments using this protocol, the inhibitory response to spermine addition occurred with some delay. We were concerned that we might be missing important dynamic information as the peak of the ratio change reported by this very sensitive probe approached saturation. We therefore performed additional experiments (Fig. 2 E) using a version of the cAMP probe ("R230K") in which the RII regulatory subunit had been engineered with a reduced affinity for cAMP (Mongillo et al., 2004). The low-affinity reporter had an estimated EC_{50} value for cAMP-dependent dissociation of PKA of ~31 μM (vs. submicromolar dissociation for the wild-type [WT] probe; Mongillo et al., 2004). Fig. 2 D also shows that the profile of cAMP reduction during CaR activation was a smooth monotonic function (typical of 13 cells in four experiments; control trace typical of 23 cells in five experiments).

In experiments similar to those in Fig. 2 D, we compared the acute action of the Ca^{2+}-mobilizing agonist carbachol on the reversal of the 480/535 emission ratio during PGE_2-stimulated cAMP production, as measured with the R230K low-affinity probe (Fig. 2 F; $n = 29$ cells in four experiments). The inhibitory action of carbachol was significantly less (only ~35%) than that elicited by spermine (normalized rate of decline –0.006 ± 0.001 SD for carbachol vs. –0.017 ± 0.001 SD during spermine; $P < 0.000001$) and occurred with a slight delay. Carbachol was also unable to completely prevent the 480/535 emission ratio increase during PGE_2 stimulation in experiments similar to those shown in Fig. 2 (A–C; and not depicted; $n = 13$ cells in two experiments). Because HEK 293 cells apparently do not express $G\alpha_i$-coupled muscarinic M2 receptors (Stope et al., 2003), we thought that the increase in intracellular Ca^{2+} elicited by carbachol stimulation might account for the modest inhibitory action seen in these experiments.

Reciprocal modulation of cAMP and Ca^{2+} pathways

Parallel experiments were performed with fura-2–loaded HEK CaR cells to examine whether PGE_2 had any effect on the pattern of intracellular Ca^{2+} signaling. CaR stimulation elicits robust and long-lasting oscillations in $[Ca^{2+}]_i$ (Breitwieser and Gama, 2001; Young and Rozengurt, 2002; De Luisi and Hofer, 2003). As shown in Fig. 3 A, stimulation with spermine alone gave rise to Ca^{2+} oscillations with a frequency of 1.78 ± 0.03 per minute ($n = 122$ cells in four experiments). This frequency was dramatically increased after acute PGE_2 addition (2.27 ± 0.06; $P < 0.0001$), until the spikes fused into an elevated plateau after ~2 min (1.85 ± 0.08 min). A third exposure to spermine after PGE_2 washout elicited oscillations that were faster than the control (2.41 ± 0.05; $P < 0.0001$, compared with the first stimulation), indicating that the effect of PGE_2 was somewhat prolonged. The amplitude of the spikes was also significantly affected by PGE_2, with the overall effect being an increased delivery of Ca^{2+} to the cytoplasm. As shown in Fig. 3 B, a 3-min preexposure to PGE_2 (when [cAMP] is typically near its maximum; see Fig. 2 D) dramatically changed the profile of the spermine response. We observed a few initial rapid spikes, which eventually fused into a prolonged plateau after 2.2 ± 0.13 min ($n = 118$ cells in four experiments). A third challenge with spermine yielded a persistent effect on oscillation frequency compared with the first control stimulation (2.03 ± 0.03 spikes per minute in control vs. 2.66 ± 0.04 for third stimulation; $P < 0.0001$). Similar results were obtained when carbachol was used in place of spermine (not depicted; $n = 90$ cells in four experiments). Although the carbachol-stimulated Ca^{2+} oscillations under control conditions were typically much less robust than those observed during spermine stimulation, the pattern of initial increase in oscillation frequency that fused into a sustained plateau was still dependably observed. Fig. 3 C shows that the frequency of oscillations recorded during three sequential control stimulations with spermine were very consistent ($n = 87$ cells in four experiments; no statistical difference). The data on oscillation frequency are summarized in Fig. 3 D.

Results very similar to those shown in Fig. 3 (A and B) were obtained when cAMP was elevated by a variety of means using 100 nM VIP (2.13 ± 0.05 oscillations per minute in control vs. 2.41 ± 0.08 with VIP; $n = 51$ cells; $P < 0.001$), 100 nM isoproterenol (2.22 ± 0.05 oscillations per minute in control vs. 2.63 ± 0.08 with isoproterenol; $n = 63$ cells; $P < 0.0001$), or 100 μM forskolin (2.34 ± 0.07 oscillations per minute in control vs. 2.70 ± 0.10 with forskolin after third stimulation; $n = 60$ cells; $P < 0.003$). Experiments with the membrane-permeable cAMP analogue Sp-8-Br-cAMPS suggest that cAMP elevation by itself and not other elements of the signal transduction cascade proximal to cAMP production were sufficient for the enhancement of Ca^{2+} signaling. 200 μM of the "potent" cAMP analogue Sp-8-Br-cAMPS caused the cAMP/FRET ratio to increase, albeit very slowly compared with native cAMP-generating agonists (not depicted; $n = 31$ cells in five experiments). Repeating the same maneuver in experiments with fura-2–loaded cells showed that acute addition of Sp-8-Br-cAMPS during Ca^{2+} spiking was able to reproduce the effect induced by PGE_2 shown in Fig. 3 (1.94 ± 0.02 spikes per minute in control vs. 2.69 ± 0.03 in the presence of cAMP analogue; $n = 135$ cells in four experiments; $P < 0.00001$). Similar effects were achieved when cells were treated with Sp-8-Br-cAMPS before spermine stimulation (not depicted; 2.16 ± 0.04 spikes per minute in control vs. 2.73 ± 0.04 in the presence of cAMP analogue; $n = 102$ cells in four experiments; $P < 0.000001$).

We did not examine in detail the mechanisms accounting for the ability of cAMP to potentiate spermine or carbachol-stimulated Ca^{2+} signaling in HEK CaR cells. This phenomenon may derive from increased excitability of the $InsP_3$ receptor because of PKA phosphorylation (for review see Bruce et al., 2003), as described previously in parotid acinar cells (Bruce et al., 2002). However, as shown in the subsequent sections, the

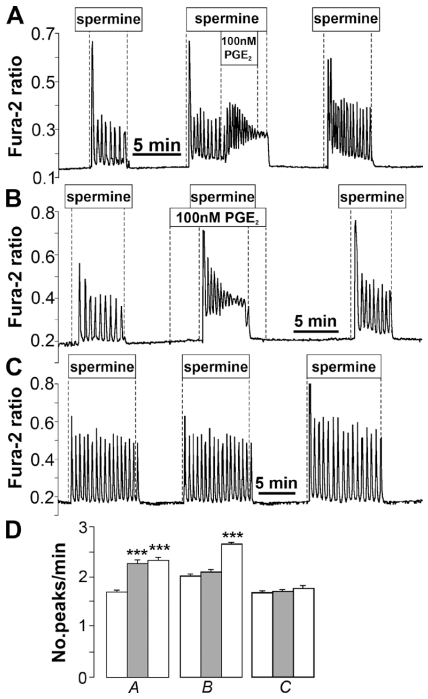

Figure 3. **Stimulation of cAMP-generating pathways alters CaR-mediated intracellular Ca^{2+} oscillations as measured by fura-2 in HEK CaR cells.** (A) Spermine-stimulated Ca^{2+} oscillations (1 mM spermine) are significantly enhanced in frequency and amplitude by acute addition of PGE_2. (B) PGE_2 pretreatment converts the oscillatory spiking pattern into a pattern of a large spike followed by several rapid oscillations that fuse into a sustained plateau. (C) Consistent spiking pattern after three consecutive control stimulations with spermine. (D) Summary of oscillation frequency data (peaks per minute ± SEM) corresponding to experimental protocols shown in A–C. The left bar represents the first spermine stimulation; the middle, gray bar represents the second stimulation; and the right bar represents the third stimulation. ***, $P < 0.0001$.

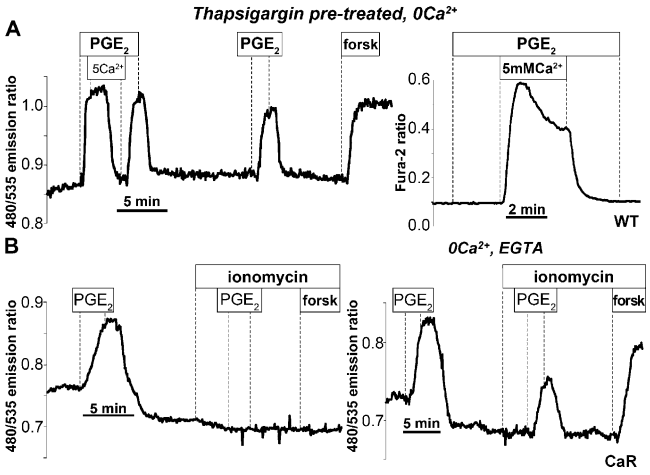

Figure 4. **Cyclic AMP accumulation is sensitive to $[Ca^{2+}]_i$.** The 480/535 nm emission ratio of the cAMP/FRET probe. (A) HEK WT cells. An artificial pulse of intracellular Ca^{2+} was generated by pretreating cells with thapsigargin in Ca^{2+}-free solutions and then re-adding 5 mM Ca^{2+} at the time point indicated during the 100-nM PGE_2 response (left). The corresponding time course for the $[Ca^{2+}]_i$ increase as measured in separate experiments by fura-2 is shown in the right panel. (B) HEK CaR cells. (left) Persistent elevation of $[Ca^{2+}]_i$ using 10 μM ionomycin in the presence of extracellular Ca^{2+} yields a persistent increase in $[Ca^{2+}]_i$ (not depicted) that inhibits both PGE_2- and forskolin-induced increases in the cAMP/FRET ratio. (right) Transient increase $[Ca^{2+}]_i$ generated by ionomycin treatment in Ca^{2+}-free solutions (not depicted) does not prevent PGE_2- or forskolin-induced increases in the cAMP/FRET ratio.

conversion to a pattern of sustained Ca^{2+} delivery in the presence of cAMP has important implications for the regulatory feedback of Ca^{2+} on cAMP signaling.

Elevation of intracellular Ca^{2+} affects cAMP production

In the parathyroid gland and some other cell models, CaR is a pleiotropic receptor that can simultaneously increase $[Ca^{2+}]_i$ and inhibit cAMP formation via $G\alpha_i$. The data of Fig. 2 F provided some initial hints that intracellular Ca^{2+} may influence cAMP levels in HEK cells. We next attempted to dissect the relative contributions of Ca^{2+} signaling and putative $G\alpha_i$-dependent actions on CaR-mediated inhibition of cAMP production in HEK 293 cells.

We first examined the actions of a large, single, "artificial" pulse of $[Ca^{2+}]_i$ on cAMP formation in HEK 293 WT cells, which do not express CaR. Before the start of the experiment, WT cells were treated with the irreversible sarco/endoplasmic reticulum Ca^{2+}-ATPase pump inhibitor thapsigargin to deplete intracellular Ca^{2+} stores. Cells were initially maintained in Ca^{2+}-free solution. Under these conditions, it is expected that readmission of Ca^{2+} to the bath will provoke a large entry of Ca^{2+} into the cell because of influx through capacitative Ca^{2+} entry pathways (Berridge et al., 2000). Parallel experiments with fura-2 showed that addition of 5 mM Ca^{2+} resulted in a large increase in $[Ca^{2+}]_i$ (Fig. 4 A, right), comparable in amplitude with the initial peak of the agonist-evoked Ca^{2+} spike ($n = 110$ cells in four experiments). In measurements using the PKA-FRET indicator under the same conditions, 5 mM Ca^{2+} administered during the peak of PGE_2-stimulated cAMP production (100 nM PGE_2) completely and reversibly decreased the ratio increase (Fig. 4 A; $n = 28$ cells in six experiments), although with a small delay.

We found similar results when we used a different experimental protocol to generate a persistent increase in $[Ca^{2+}]_i$ in HEK 293 CaR cells. 10 μM ionomycin, a Ca^{2+} ionophore that releases internal Ca^{2+} stores and promotes Ca^{2+} entry from the extracellular space (as well as activates store-operated channels via store depletion), was able to completely abolish both PGE_2- and forskolin-induced cAMP elevations, but only in the presence of external Ca^{2+} (Fig. 4 B, left; $n = 28$ cells in four experiments). As shown in Fig. 4 B (right), however, the responses to both PGE_2 and forskolin were evident during ionomycin treatment in the absence of external Ca^{2+} ($n = 28$ cells in four experiments). Under these conditions, ionomycin is expected to yield only a transient (~2-min duration) increase in intracellular Ca^{2+} because of store release. These experiments confirm that intracellular Ca^{2+} was indeed able to effectively modulate cAMP levels in HEK 293 cells and are in agreement with previous reports that Ca^{2+} entering the cell via store-operated channels preferentially regulates cAMP production by AC (Cooper, 2003). This explanation is also consistent with the data shown in Fig. 2 F, in which acute stimulation with the

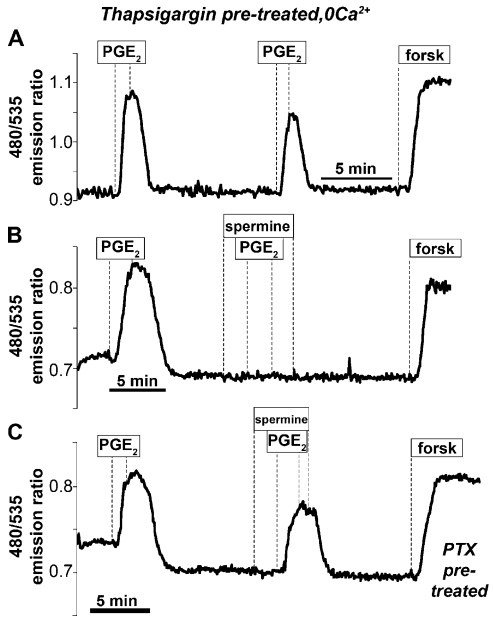

Figure 5. **CaR inhibits cAMP production through PTX-sensitive $G\alpha_i$.** Measurements of the 480/535 nm emission ratio of the PKA-based sensor were performed in thapsigargin-pretreated HEK CaR cells maintained in Ca^{2+}-free solutions (to eliminate contributions from Ca^{2+} signaling). (A) Control experiment showing two successive responses to 100 nM PGE_2 followed by maximal response to 100 μM forskolin. (B) 1 mM spermine prevents PGE_2-induced ratio elevation in the absence of Ca^{2+} signaling. (C) Pretreatment with PTX rescues the PGE_2 response, in spite of the presence of spermine.

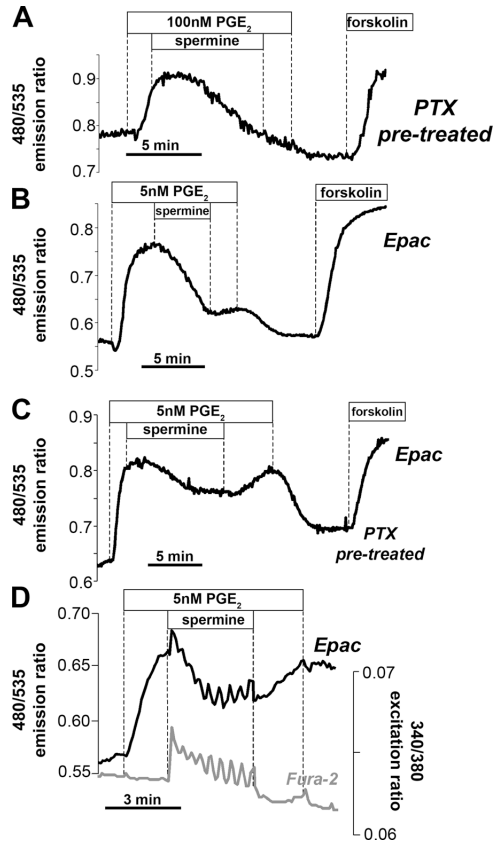

Figure 6. **Profile of the spermine-induced decline in cAMP after PTX pretreatment as measured by PKA- and Epac-based sensors.** (A) In PTX-pretreated HEK CaR cells (100 ng/ml × 16 h), spermine added during the peak of PGE_2 stimulation causes a smooth decline in the 480/535 nm ratio, even though $[Ca^{2+}]_i$, as measured by fura-2, initially maintains an oscillatory pattern under these conditions (not depicted). (B) A similar smooth decline in the 480/535 nm emission ratio is observed when spermine is added during the peak of the response to 5 nM PGE_2 as measured using the Epac sensor. (C) As in B, but in PTX-pretreated cells. (D) Concurrent fura-2 and FRET ratio measured in fura-2–loaded HEK CaR cells transfected with the Epac sensor shows persistence of spermine-stimulated Ca^{2+} oscillations in Epac-expressing cells, although there is significant optical contamination of the FRET channel by the fura-2 signal.

Ca^{2+}-mobilizing agonist carbachol inhibited the cAMP signal, although this inhibition was diminished significantly compared with the potent actions of spermine.

The ability of CaR to block cAMP production is PTX sensitive

We used the specific blocker of $G\alpha_i$, PTX, to determine whether CaR expressed in HEK cells could also inhibit cAMP production through this pathway. Previous attempts to characterize this aspect of CaR signaling in HEK CaR cells using conventional radioimmune assays for cAMP have been only partially successful (Chang et al., 1998). During these experiments we eliminated the Ca^{2+} signaling component by pretreating the cells with thapsigargin in Ca^{2+}-free solutions. Control experiments (Fig. 5 A) demonstrate that store-depleted HEK CaR cells maintained in Ca^{2+}-free solutions were still able to repeatedly respond to PGE_2 and forskolin (n = 37/39 cells in six experiments). Somewhat surprisingly, this response was entirely abolished by spermine (Fig. 5 B; n = 28/29 cells in four experiments). This implies that activation of CaR is capable of regulating cAMP signaling through a pathway entirely independent of Ca^{2+}. However, the response to PGE_2 was recovered in the presence of spermine when $G\alpha_i$, the link between CaR and AC inactivation, was inhibited by PTX (n = 19 cells in five experiments; Fig. 5 C).

The preceding results demonstrate that CaR exerts a dual action on cAMP signaling, working through intracellular Ca^{2+} and PTX-sensitive pathways. Based on the strong oscillatory pattern of the Ca^{2+} signal (Fig. 3, A–C), we wondered if conditions existed under which cAMP would also display a complex oscillatory or descending "staircase" profile. Such cAMP oscillations might arise from repetitive coupling of CaR to AC via $G\alpha_i$, or as a secondary consequence of intracellular Ca^{2+} spiking.

Fig. 6 A shows that in the absence of $G\alpha_i$-mediated inhibition (PTX pretreatment), spermine still caused a smooth monotonic reduction in the FRET ratio (compare with control in Fig. 2 E), and this occurred with a substantial delay (n = 20 cells in four experiments). We expected to see fluctuations or stepwise decrements in cAMP because parallel experiments in fura-2–loaded cells revealed initial persistence of Ca^{2+} oscillations (similar to those observed in Fig. 3; not depicted) after PTX treatment, and the data of Fig. 5 showed cAMP accumulation to be very sensitive to intracellular Ca^{2+}. We considered the possibility that the PKA-based sensors we were using had not been fast enough to resolve rapid fluctuations in cAMP because a relatively complex binding reaction involving four cAMP

molecules and the dissociation of four PKA subunits is required to see a change in FRET. However, a similar profile was observed in experiments using the fast monomeric Epac-based sensor described on the previous page. As shown in Fig. 6 B, spermine addition during stimulation of cells with a low dose (5 nM) of PGE_2 caused a smooth reversible decline in the FRET ratio. Fig. 6 C illustrates the powerful inhibitory effect of the PTX-sensitive component of CaR stimulation on cAMP signaling. After PTX pretreatment, the action of spermine-induced Ca^{2+} signals can be examined in isolation. A smooth, slow decline in the FRET ratio that occurred with a notable delay was observed upon spermine addition. Concurrent measurements of the 340:380 nm fura-2 excitation ratio and 480/535 nm FRET emission ratio in fura-2–loaded HEK CaR cells expressing the Epac sensor confirmed that the presence of Epac did not alter Ca^{2+} oscillations (Fig. 6 D). However, we noted significant "bleed through" of the fura-2 signal into the FRET channels (see Materials and methods for details), giving rise to apparent oscillations in the FRET ratio that were never observed in cells not loaded with fura-2 ($n = 9$ cells in five experiments).

In numerous experiments using the protocols shown in Fig. 2 (A–F; on hundreds of individual cells) using both low-affinity WT PKA-based indicators and varying doses and combinations of receptor agonists, we observed only a regular, uniform decline in the ratio after CaR activation. The question remains, why are fluctuations in the FRET ratio, driven by intracellular Ca^{2+} spikes, not evident in these experiments? The following data show that the frequency and duration of Ca^{2+} spiking are critical determinants of whether the inhibitory actions of intracellular Ca^{2+} are translated to the cAMP signaling pathway.

We generated repetitive artificial Ca^{2+} spikes in HEK WT cells using a pattern that mimicked spermine-stimulated Ca^{2+} oscillations in HEK CaR cells. WT cells were pretreated with thapsigargin in Ca^{2+}-free solutions, and intermittent pulses of Ca^{2+} (1 mM) were applied during PGE_2-stimulated cAMP accumulation. As shown in Fig. 7 A, with a frequency of one Ca^{2+} spike (lasting 1 min) every 2 min, no effect could be discerned on the FRET ratio ($n = 8$ cells in three experiments). Fig. 7 B shows that the low-affinity PKA-based indicator should, in principle, be able to respond to alterations in [cAMP] on the minute time scale. In these experiments, cells were permeabilized with digitonin in an intracellular-like buffer. Cells were then alternately superfused for 1-min pulses with solutions containing 30 or 50 μM cAMP ($n = 9$ cells in four experiments). These seemingly high concentrations of cAMP were used because in situ calibration of the low-affinity probe revealed this to be the range of [cAMP] levels achieved during stimulation with 500 nM PGE_2 (not depicted; $n = 12$ cells in five experiments). In contrast to the results of Fig. 7 A, when the frequency and duration of the Ca^{2+} pulses were altered (one 3-min-long spike every 6 min), distinctive stepwise reductions in Ca^{2+} were evident (Fig. 7 C; $n = 22$ cells in five experiments). It was consistently observed that >1 min was required after admission of Ca^{2+} in the superfusion before the FRET ratio began to decline (during the first Ca^{2+} pulse, the ratio started to decrease only after 1.63 ± 0.60 min, for the second Ca^{2+} pulse, after 1.40 ± 0.66 min, and for the third pulse, after 1.22 ± 0.70 min; $n = 22$ cells in five experiments), explaining why the pattern of rapid Ca^{2+} spiking in Fig. 7 A failed to elicit any effect. These results indicate that in this model system the cAMP machinery is immune to rapid Ca^{2+} spiking but does respond to large static increases in Ca^{2+} (as sensed by PKA and Epac), which sets cAMP at a new, reduced level.

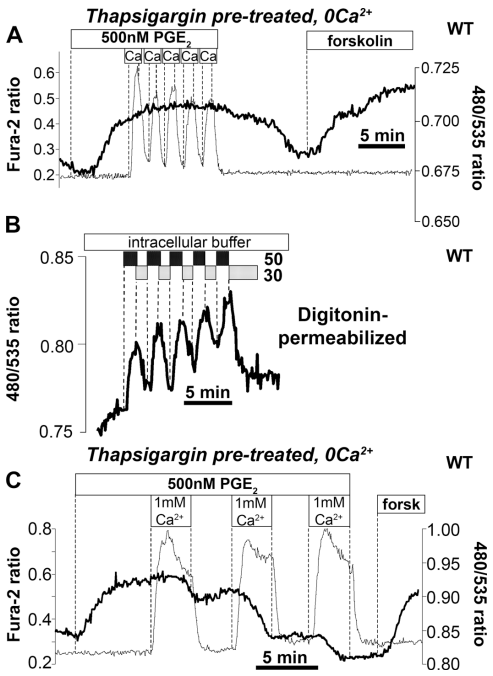

Figure 7. **PKA dissociation is immune to high-frequency Ca^{2+} oscillations.** Parallel measurements of $[Ca^{2+}]_i$ using fura-2 and cAMP using the low-affinity R230K version of the PKA/FRET probe in HEK WT cells. (A) Effect of high-frequency artificial Ca^{2+} pulses during peak of PGE_2 response in cells preincubated in thapsigargin/Ca^{2+}-free solutions. (B) Control experiment in digitonin-permeabilized WT cells alternately superfused with 50 and 30 μM cAMP for 1 min each shows the response time of the probe to rapid fluctuations in [cAMP]. (C) Low-frequency, long-duration Ca^{2+} pulses generate complex staircase patterns of cAMP in HEK WT cells.

Discussion

In vivo, cells are bombarded with a variety of extracellular first messengers that may have complementary or antagonistic actions. These stimuli must be integrated dependably at the level of intracellular second messenger cascades if the appropriate biological endpoint is to be achieved. In addition, although there are many specific cell-surface receptors, there are relatively few second messengers. An emerging concept in the field of signal transduction is the existence of signaling networks that exploit complex spatiotemporal patterns of second messenger molecules, allowing encoding of an expanded repertoire of messages using limited numbers of messengers (Zaccolo and Pozzan, 2003).

In this study we examined the interactions of the widely expressed GPCR, CaR, with other receptors linked to cAMP generation. Our data show that in HEK cells, CaR is exceptionally competent in terminating cAMP signaling initiated by the inflammatory mediator PGE_2 (Figs. 2 and 6) as well as cAMP

signals generated by isoproterenol and VIP (not depicted). The reasons for this potent action are threefold. First is the somewhat predictable inhibition through the classical PTX-sensitive $G\alpha_i$ pathway that we demonstrated here to be very effective by itself in HEK CaR cells (Figs. 5 and 6). Although it was known from prior biochemical studies that CaR is able to interact with $G\alpha_i$ in several cell types, the use of sensitive FRET-based imaging techniques allowed us to examine this interaction with unprecedented spatiotemporal detail in single living cells. The second reason CaR stimulation is so efficient in preventing or reversing cAMP signaling is that it activates intracellular Ca^{2+} signaling cascades. Our data demonstrate that cAMP accumulation was sensitive to $[Ca^{2+}]_i$ in HEK cells (Fig. 4), as has been described previously for other cell models. Under control conditions, these Ca^{2+} signals are manifested as oscillations, which persist with very little desensitization as long as CaR agonists are present. However, in the presence of cAMP, this oscillatory pattern of Ca^{2+} signaling was ultimately converted to a larger, sustained Ca^{2+} elevation that was shown here to be much more effective in modulating cAMP levels (Figs. 3 and 4). This enhancement of the Ca^{2+} signal by cAMP constitutes the third mechanism that serves to reinforce the prompt termination of the cAMP elevation in HEK CaR cells.

CaR and other receptors that are able to interact through both $G\alpha_i$ and Ca^{2+} may be useful targets for pharmacological control of cAMP signaling in several tissues. Of course, it must be kept in mind that the action of Ca^{2+} on cAMP signaling will depend strongly on the particular repertoire of PDE and AC isoforms expressed in a given cell type and whether they are activated, unaffected, or inhibited by Ca^{2+} (Cooper et al., 1995; for review see Bruce et al., 2003). Landa et al. (2005) recently provided evidence for rapid Ca^{2+}-dependent augmentation of cAMP signaling using Epac-based cAMP sensors in insulin-secreting MIN6 β cells, a cell type that expresses a very different panel of ACs and PDEs. de Jesus Ferreira et al. (1998) described coexpression of Ca^{2+}-inhibitable (type 6) AC and CaR in the cortical thick ascending limb of the kidney and further showed potent antagonism of cAMP signaling during CaR stimulation by physiological levels of extracellular $[Ca^{2+}]$. CaR is also known to be concentrated in neuronal synapses, where predictions from modelling and direct measurements have shown significant depletions in extracellular $[Ca^{2+}]$ during neuronal activity because of entry though voltage-operated Ca^{2+} channels (Egelman and Montague, 1999; Cohen and Fields, 2004). Under these conditions, it might be predicted that lowering extrasynaptic $[Ca^{2+}]$ would relieve repression of cAMP signaling through CaR's interaction with $G\alpha_i$ (keeping in mind, however, that Ca^{2+}-activated ACs expressed in neuronal cells might mitigate this effect). This type of regulation could have profound implications for learning and memory. We recently provided functional evidence that physiological fluctuations in extracellular $[Ca^{2+}]$ can affect the secretory activity of the intact gastric mucosa through a PTX-sensitive interaction of CaR with the cAMP signaling pathway (Caroppo et al., 2004). We termed this effect the "third messenger" action of Ca^{2+} because CaR activation resulted from dynamic extracellular $[Ca^{2+}]$ fluctuations secondary to stimulation of the tissue with a Ca^{2+}-mobilizing cholinergic agonist. Interestingly, as has been reported in several other cell systems, direct CaR stimulation did not produce an intracellular Ca^{2+} signal in gastric cells (Hofer et al., 2004). These findings highlight the complexity of signaling networks in vivo, where the effects of $[Ca^{2+}]$ changes in both intracellular and extracellular compartments must be taken into account in tissues where CaR or other Ca^{2+} sensors are expressed.

We undertook this study with the initial expectation that cAMP, as reported by cAMP-dependent conformational changes of two major cellular targets of the cAMP signal, PKA and Epac, might undergo "oscillations" or other dynamic fluctuations during concurrent stimulation of CaR and other cAMP-generating receptors, based on the robust oscillatory Ca^{2+} response during CaR activation in HEK CaR cells. Gorbunova and Spitzer (2002) reported slow, spontaneous cAMP transients lasting several minutes in embryonic *Xenopus laevis* spinal neurons that followed bursts of spontaneous Ca^{2+} oscillations. These investigators identified optimal patterns of Ca^{2+} spiking during the preceding cluster of Ca^{2+} oscillations that gave rise to these intermittent cAMP elevations. We examined the cAMP signal over a much shorter time frame and only during contemporaneous stimulation of CaR and cAMP pathways. In our studies we only observed a smooth monotonic decline in the FRET ratio under these conditions. We cannot exclude the possibility that complex spatiotemporal cAMP dynamics occur in localized domains (Tasken and Aandahl, 2004) and are therefore undetectable by the PKA- or Epac-based sensors. Rich et al. (2001a) provided evidence for localized cAMP signals under the plasma membrane of HEK cells that differed temporally from those of the bulk cytoplasm, as measured by currents through transfected cyclic nucleotide gated cation channels. However, our data clearly show that the relatively fast frequencies of Ca^{2+} oscillations that are typical of stimulation with native Ca^{2+}-mobilizing agonists cannot exert effects on PKA subunit dissociation (Fig. 7 A) or Epac conformational changes (Fig. 6, B and C). This important result means that, in principle, high-frequency Ca^{2+} signaling can take place without affecting the activity of two of the major targets of the intracellular cAMP signal, PKA and Epac.

Our data revealed a complex twist to this story, namely, that during concurrent stimulation of cAMP and Ca^{2+} pathways, cAMP initially causes the Ca^{2+} oscillation frequency to increase. However, these spikes eventually fuse into a persistent Ca^{2+} elevation, a pattern that is effective in inhibiting cAMP accumulation. This may help explain why the effects of Ca^{2+}-mobilizing agonists (spermine and carbachol) on the FRET ratio are only evident in Fig. 2 F and Fig. 6 (A and C) after some delay. Initially, rapid Ca^{2+} spiking would not be effective in turning off cAMP production, but after several minutes, during the elevated plateau phase of the signal, Ca^{2+} would be able to exert its inhibitory action on cAMP.

Application of artificial low-frequency, long-duration signals yielded a complex staircase profile of cAMP decline (Fig. 7 C). This mode of low-frequency, long-duration Ca^{2+} spiking has not been observed in this cell type during a single stimulation with a native agonist; however, this profile would be generated

during a brief (~3-min duration) stimulation with a Ca^{2+}-mobilizing agonist in the presence of cAMP. Because the molecular targets of cAMP (e.g., type I and II regulatory subunits of PKA and Epac) have a wide range of affinities for cAMP, it is possible that a large uniform Ca^{2+} pulse of moderate duration could serve to "reset" [cAMP] to a lower level that favors activation of a higher affinity cAMP-binding target. This may be one more example of how complex spatial and temporal interactions between different signaling systems can be used to create unique messenger profiles that elicit diverse biological endpoints.

Materials and methods

Cell culture

HEK 293 cells stably expressing the human CaR and WT HEK 293 were grown in high-glucose DME + glutamax (Life Technologies) supplemented with 10% FBS containing 10 U/ml penicillin and 10 mg/ml streptomycin. Cells were maintained in a humidified incubator under 5% CO_2 and 95% O_2 at 37°C.

FRET-based measurement of cAMP in single cells

Intracellular cAMP was imaged in single cells expressing a genetically encoded FRET-based indicator described previously (Zaccolo and Pozzan, 2002; Zaccolo, 2004). In brief, the probe was generated by fusing the regulatory and the catalytic subunits of PKA to CFP and YFP, respectively. When [cAMP] is low, PKA is in its holomeric form and the two fluorophores, CFP and YFP, are separated physically by a few nanometers. The excitation energy of the CFP ("donor," 440 nm) can pass via Förster energy transfer to the acceptor molecule, YFP, which in turn emits at its own wavelength (535 nm). This gives rise to maximal FRET. When intracellular cAMP rises, the two PKA subunits dissociate and FRET is abolished. FRET can be estimated as the ratio of donor (480 nm) to acceptor emission (535 nm) intensities when cells are excited at the donor excitation wavelength (440 nm). Changes in the fluorescence emission ratio (480/535 nm) are directly correlated to changes in catalytic and regulatory subunit association and thus to cAMP levels (Mongillo et al., 2004).

A second type of sensor for cAMP relying on the cAMP-dependent conformational change of the monomeric cAMP-binding protein Epac (monitored as a change in FRET between CFP- and YFP-labeled domains) was also used. CFP-Epac(∂DEP)-YFP, a catalytically inactive version of the cAMP effector protein Epac with a cytosolic localization (Ponsioen et al., 2004), was a gift from K. Jalink and colleagues (the Netherlands Cancer Institute, Amsterdam, Netherlands). The 480/535 nm emission ratio (excitation at 440 nm) of this fast cAMP sensor was monitored as for the PKA-based probes.

HEK 293 CaR and HEK 293 WT cells were plated onto sterilized glass coverslips resting in the bottom of 60-mm plastic culture dishes and transiently transfected with cAMP probes using effectene transfection reagent (QIAGEN). Imaging experiments were performed on subconfluent cells 2 d after the transfection using a ratio imaging setup running Metafluor software (Universal Imaging Corp.). Coverslips with probe-transfected cells were mounted in an open-topped perfusion chamber (Series 20; Warner Instrument Corp.) and placed on the heated stage of an inverted microscope (TE200; Nikon) equipped with a CFP/YFP FRET filter set (XF88-2/E; Omega Optical). Cells were excited at 440 nm for 80 ms through a 40× (NA 1.4) oil immersion objective (455-nm DRLP). Emitted light was captured alternately at 480 and 535 nm using a microprocessor-controlled filter wheel placed in the emission light path. Pairs of fluorescence images at the two wavelengths were captured by a charge-coupled device camera (ORCA ER; Hamamatsu) every 5 s and converted to a ratio image by the Metafluor software.

Measurement of $[Ca^{2+}]_i$

Parallel measurements of cytoplasmic-free $[Ca^{2+}]$ were performed using fura-2–AM–loaded HEK 293 cells as described previously (De Luisi and Hofer, 2003). Using the imaging system described for cAMP, cells were excited alternately at 340 and 380 nm for 80 ms through a 40× (NA 1.4) oil immersion objective. The excitation wavelengths were generated using a computer-controlled filter wheel (Sutter Instrument Co.) placed in the path of a 100-W mercury light source. Pairs of fluorescence images (emission collected >510 nm) were captured by the charge-coupled device camera every 4 s and converted to a ratio image by the Metafluor software.

Concurrent measurements of fura-2 and CFP-YFP FRET

HEK CaR cells expressing the Epac sensor were loaded with fura-2 and sequential fura-2, and CFP/YFP ratio pairs were collected, keeping only the 455-nm dichroic mirror in place (Landa et al., 2005). Significant contamination of the FRET ratio with the fura-2 signal was noted using this configuration.

Experiments on digitonin-permeabilized HEK cells expressing R230K PKA-based sensor

As described previously (Hofer and Machen, 1993), cells were rinsed briefly in a high K^+ solution (125 mM KCl, 25 mM NaCl, 0.1 mM $MgCl_2$, and 10 mM Hepes, pH 7.20) and then exposed for 2–3 min to an intracellular buffer (the same solution with free $[Ca^{2+}]$ clamped to 170 nM using Ca^{2+}/EGTA buffers and supplemented with 1 mM Na_2ATP) also containing 5 μg/ml digitonin at 37°C. After plasma membrane permeabilization, cells were continuously superfused with intracellular buffer (without digitonin, but containing varying [cAMP]). An in situ calibration established that 500 nM PGE_2 caused cAMP levels to increase to ~30–50 μM, as measured by the low-affinity R230K sensor.

Solutions and materials

Unless otherwise stated, all chemicals were purchased from Sigma-Aldrich. Experiments were performed with a Ringer's solution containing 121 mM NaCl, 2.4 mM K_2HPO_4, 0.4 mM KH_2PO_4, 1.2 mM $CaCl_2$, 1.2 mM $MgCl_2$, 10 mM glucose, and 10 mM Hepes/NaOH, pH 7.40. Bradykinin, ionomycin, and Sp-8-Br-cAMPS (adenosine 3′, 5′-cyclic monophosphorthioate, 8-Bromo, Sp-Isomer, and Na^+ salt) were obtained from Calbiochem-Novabiochem; fura-2–AM and BAPTA-AM were obtained from Invitrogen. NPS-R-467 was obtained from E. Nemeth (NPS Pharmaceuticals, Salt Lake City, UT). When DMSO or ethanol was used as a solvent, the final solvent concentration never exceeded 0.01 or 0.1%, respectively.

Statistical analysis

At the end of each experiment using the cAMP probes, cells were superfused with a supramaximal dose (50–100 μM) of forskolin, a reliable activator of AC. Because cells were occasionally fluorescent but nevertheless nonresponsive to agonists (possibly because of improper folding or targeting of the probe), only the cells that responded to the forskolin with a robust ratio increase were statistically averaged. Statistical significance was determined using a paired *t* test. Data from several cells in a particular experimental run were averaged, and experiment averages were used to calculate the mean ± SEM. Traces shown are typical of at least three similar experiments unless otherwise noted.

We are very grateful to Dr. Kees Jalink for the kind gift of the Epac sensor. We also thank Jessica Roy for expert technical assistance, Professor Edward M. Brown for helpful comments on our data, and Dr. Ed Nemeth for graciously providing us with NPS-R-467.

These studies were supported by grants from the Medical Research Service of the Veteran's Administration and a pilot/feasibility award from the Brigham and Women's Surgical Research Group (both to A.M. Hofer). A. Gerbino was supported by a doctoral fellowship awarded jointly from the University of Bari and the European Community (FSE). Work in the laboratory of M. Zaccolo is supported by Telethon Italy (TCP00089), the European Union (QLK3-CT-2002-02149), the Italian Cystic Fibrosis Research Foundation, and the Fondazione Compagnia di San Paolo.

Submitted: 12 July 2005
Accepted: 16 September 2005

References

Adams, S.R., A.T. Harootunian, Y.J. Buechler, S.S. Taylor, and R.Y. Tsien. 1991. Fluorescence ratio imaging of cyclic AMP in single cells. *Nature.* 349:694–697.

Beavo, J.A., and L.L. Brunton. 2002. Cyclic nucleotide research—still expanding after half a century. *Nat. Rev. Mol. Cell Biol.* 3:710–718.

Berridge, M.J., P. Lipp, and M.D. Bootman. 2000. The versatility and universality of calcium signalling. *Nat. Rev. Mol. Cell Biol.* 1:11–21.

Breitwieser, G.E., and L. Gama. 2001. Calcium-sensing receptor activation induces intracellular calcium oscillations. *Am. J. Physiol. Cell Physiol.* 280:C1412–C1421.

Breitwieser, G.E., S.U. Miedlich, and M. Zhang. 2004. Calcium sensing receptors as integrators of multiple metabolic signals. *Cell Calcium.* 35:209–216.

Brown, E.M., and R.J. MacLeod. 2001. Extracellular calcium sensing and extra-

cellular calcium signaling. *Physiol. Rev.* 81:239–297.

Brown, E.M., G. Gamba, D. Riccardi, M. Lombardi, R. Butters, O. Kifor, A. Sun, M.A. Hediger, J. Lytton, and S.C. Hebert. 1993. Cloning and characterization of an extracellular Ca(2+)-sensing receptor from bovine parathyroid. *Nature.* 366:575–580.

Bruce, J.I., T.J. Shuttleworth, D.R. Giovannucci, and D.I. Yule. 2002. Phosphorylation of inositol 1,4,5-trisphosphate receptors in parotid acinar cells. A mechanism for the synergistic effects of cAMP on Ca2+ signaling. *J. Biol. Chem.* 277:1340–1348.

Bruce, J.I., S.V. Straub, and D.I. Yule. 2003. Crosstalk between cAMP and Ca2+ signaling in non-excitable cells. *Cell Calcium.* 34:431–444.

Caroppo, R., A. Gerbino, G. Fistetto, M. Colella, L. Debellis, A.M. Hofer, and S. Curci. 2004. Extracellular calcium acts as a "third messenger" to regulate enzyme and alkaline secretion. *J. Cell Biol.* 166:111–119.

Chabardes, D., M. Imbert-Teboul, and J.M. Elalouf. 1999. Functional properties of Ca2+-inhibitable type 5 and type 6 adenylyl cyclases and role of Ca2+ increase in the inhibition of intracellular cAMP content. *Cell. Signal.* 11:651–663.

Chang, W., S. Pratt, T.H. Chen, E. Nemeth, Z. Huang, and D. Shoback. 1998. Coupling of calcium receptors to inositol phosphate and cyclic AMP generation in mammalian cells and *Xenopus laevis* oocytes and immunodetection of receptor protein by region-specific antipeptide antisera. *J. Bone Miner. Res.* 13:570–580.

Chen, C.J., J.V. Barnett, D.A. Congo, and E.M. Brown. 1989. Divalent cations suppress 3′,5′-adenosine monophosphate accumulation by stimulating a pertussis toxin-sensitive guanine nucleotide-binding protein in cultured bovine parathyroid cells. *Endocrinology.* 124:233–239.

Cohen, J.E., and R.D. Fields. 2004. Extracellular calcium depletion in synaptic transmission. *Neuroscientist.* 10:12–17.

Conigrave, A.D., S.J. Quinn, and E.M. Brown. 2000. Cooperative multi-modal sensing and therapeutic implications of the extracellular Ca(2+) sensing receptor. *Trends Pharmacol. Sci.* 21:401–407.

Cooper, D.M. 2003. Molecular and cellular requirements for the regulation of adenylate cyclases by calcium. *Biochem. Soc. Trans.* 31:912–915.

Cooper, D.M., N. Mons, and J.W. Karpen. 1995. Adenylyl cyclases and the interaction between calcium and cAMP signalling. *Nature.* 374:421–424.

de Jesus Ferreira, M.C., C. Helies-Toussaint, M. Imbert-Teboul, C. Bailly, J.M. Verbavatz, A.C. Bellanger, and D. Chabardes. 1998. Co-expression of a Ca2+-inhibitable adenylyl cyclase and of a Ca2+-sensing receptor in the cortical thick ascending limb cell of the rat kidney. Inhibition of hormone-dependent cAMP accumulation by extracellular Ca2+. *J. Biol. Chem.* 273:15192–15202.

De Luisi, A., and A.M. Hofer. 2003. Evidence that Ca(2+) cycling by the plasma membrane Ca(2+)-ATPase increases the 'excitability' of the extracellular Ca(2+)-sensing receptor. *J. Cell Sci.* 116:1527–1538.

DiPilato, L.M., X. Cheng, and J. Zhang. 2004. Fluorescent indicators of cAMP and Epac activation reveal differential dynamics of cAMP signaling within discrete subcellular compartments. *Proc. Natl. Acad. Sci. USA.* 101:16513–16518.

Dolmetsch, R.E., K. Xu, and R.S. Lewis. 1998. Calcium oscillations increase the efficiency and specificity of gene expression. *Nature.* 392:933–936.

Egelman, D.M., and P.R. Montague. 1999. Calcium dynamics in the extracellular space of mammalian neural tissue. *Biophys. J.* 76:1856–1867.

Geng, W., Z. Wang, J. Zhang, B.Y. Reed, C.Y. Pak, and O.W. Moe. 2005. Cloning and characterization of the human soluble adenylyl cyclase. *Am. J. Physiol. Cell Physiol.* 288:C1305–C1316.

Goraya, T.A., N. Masada, A. Ciruela, and D.M. Cooper. 2004. Sustained entry of Ca2+ is required to activate Ca2+-calmodulin-dependent phosphodiesterase 1A. *J. Biol. Chem.* 279:40494–40504.

Gorbunova, Y.V., and N.C. Spitzer. 2002. Dynamic interactions of cyclic AMP transients and spontaneous Ca(2+) spikes. *Nature.* 418:93–96.

Hofer, A.M., and T.E. Machen. 1993. Technique for in situ measurement of calcium in intracellular inositol 1,4,5-trisphosphate-sensitive stores using the fluorescent indicator mag-fura-2. *Proc. Natl. Acad. Sci. USA.* 90:2598–2602.

Hofer, A.M., and E.M. Brown. 2003. Extracellular calcium sensing and signalling. *Nat. Rev. Mol. Cell Biol.* 4:530–538.

Hofer, A.M., A. Gerbino, R. Caroppo, and S. Curci. 2004. The extracellular calcium-sensing receptor and cell-cell signaling in epithelia. *Cell Calcium.* 35:297–306.

Hoffmann, R., G.S. Baillie, S.J. MacKenzie, S.J. Yarwood, and M.D. Houslay. 1999. The MAP kinase ERK2 inhibits the cyclic AMP-specific phosphodiesterase HSPDE4D3 by phosphorylating it at Ser579. *EMBO J.* 18:893–903.

Houslay, M.D., and G. Milligan. 1997. Tailoring cAMP-signalling responses through isoform multiplicity. *Trends Biochem. Sci.* 22:217–224.

Landa, L.R., Jr., M. Harbeck, K. Kaihara, O. Chepurny, K. Kitiphongspattana, O. Graf, V.O. Nikolaev, M.J. Lohse, G.G. Holz, and M.W. Roe. 2005. Interplay of Ca2+ and cAMP signaling in the insulin-secreting MIN6 beta-cell line. *J. Biol. Chem.* 280:31294–31302.

Ludwig, M.G., and K. Seuwen. 2002. Characterization of the human adenylyl cyclase gene family: cDNA, gene structure, and tissue distribution of the nine isoforms. *J. Recept. Signal Transduct. Res.* 22:79–110.

Mongillo, M., T. McSorley, S. Evellin, A. Sood, V. Lissandron, A. Terrin, E. Huston, A. Hannawacker, M.J. Lohse, T. Pozzan, et al. 2004. Fluorescence resonance energy transfer-based analysis of cAMP dynamics in live neonatal rat cardiac myocytes reveals distinct functions of compartmentalized phosphodiesterases. *Circ. Res.* 95:67–75.

Nemeth, E.F. 2004. Calcimimetic and calcilytic drugs: just for parathyroid cells? *Cell Calcium.* 35:283–289.

Ponsioen, B., J. Zhao, J. Riedl, F. Zwartkruis, G. van der Krogt, M. Zaccolo, W.H. Moolenaar, J.L. Bos, and K. Jalink. 2004. Detecting cAMP-induced Epac activation by fluorescence resonance energy transfer: Epac as a novel cAMP indicator. *EMBO Rep.* 5:1176–1180.

Rich, T.C., K.A. Fagan, T.E. Tse, J. Schaack, D.M. Cooper, and J.W. Karpen. 2001a. A uniform extracellular stimulus triggers distinct cAMP signals in different compartments of a simple cell. *Proc. Natl. Acad. Sci. USA.* 98:13049–13054.

Rich, T.C., T.E. Tse, J.G. Rohan, J. Schaack, and J.W. Karpen. 2001b. In vivo assessment of local phosphodiesterase activity using tailored cyclic nucleotide–gated channels as cAMP sensors. *J. Gen. Physiol.* 118:63–78.

Stope, M.B., C. Kunkel, C. Kories, M. Schmidt, and M.C. Michel. 2003. Differential agonist-induced regulation of human M2 and M3 muscarinic receptors. *Biochem. Pharmacol.* 66:2099–2105.

Tasken, K., and E.M. Aandahl. 2004. Localized effects of cAMP mediated by distinct routes of protein kinase A. *Physiol. Rev.* 84:137–167.

Thorn, P., A.M. Lawrie, P.M. Smith, D.V. Gallacher, and O.H. Petersen. 1993. Local and global cytosolic Ca2+ oscillations in exocrine cells evoked by agonists and inositol trisphosphate. *Cell.* 74:661–668.

Wayman, G.A., T.R. Hinds, and D.R. Storm. 1995. Hormone stimulation of type III adenylyl cyclase induces Ca2+ oscillations in HEK-293 cells. *J. Biol. Chem.* 270:24108–24115.

Young, S.H., and E. Rozengurt. 2002. Amino acids and Ca2+ stimulate different patterns of Ca2+ oscillations through the Ca2+-sensing receptor. *Am. J. Physiol. Cell Physiol.* 282:C1414–C1422.

Zaccolo, M. 2004. Use of chimeric fluorescent proteins and fluorescence resonance energy transfer to monitor cellular responses. *Circ. Res.* 94:866–873.

Zaccolo, M., and T. Pozzan. 2002. Discrete microdomains with high concentration of cAMP in stimulated rat neonatal cardiac myocytes. *Science.* 295:1711–1715.

Zaccolo, M., and T. Pozzan. 2003. CAMP and Ca2+ interplay: a matter of oscillation patterns. *Trends Neurosci.* 26:53–55.

Zaccolo, M., F. De Giorgi, C.Y. Cho, L. Feng, T. Knapp, P.A. Negulescu, S.S. Taylor, R.Y. Tsien, and T. Pozzan. 2000. A genetically encoded, fluorescent indicator for cyclic AMP in living cells. *Nat. Cell Biol.* 2:25–29.